

Supplementary materials for

Constructing multifunctional MOFs@rGO hydro-/aerogel by self-assembly process for customized water remediation

Jiajun Mao,^a Mingzheng Ge,^a Jianying Huang,^a Yuekun Lai,^{*a} Keqin Zhang,^a Kai Meng,^{*a} Yuxin Tang^{*b}

^aNational Engineering Laboratory for Modern Silk, College of Textile and Clothing Engineering, Soochow University, Suzhou 215123, China.

Email: yklai@suda.edu.cn (Y. Lai); mk2009@suda.edu.cn (K. Meng)

^bSchool of Materials Science and Engineering, Nanyang Technological University, 50 Nanyang Avenue, 639798, Singapore.

Email: tang0212@ntu.edu.sg (Y. Tang)

Table of contents

1. Supporting Movies

Movie 1. Repeated oil-water separation by ZIF-8/rGA.

Movie 2. Magnetic Fe₃O₄/rGA.

Movie 3. Elastic ZIF-8/rGA.

Movie 4. Electric Fe₃O₄/rGA.

2. Supporting note for fabrication process of MOFs@rGA and rGA@metal oxides:

Zn²⁺/rGA: 12 mL of 1 mg mL⁻¹ GO aqueous solution and 12 μL hydrazine hydrate (or 120 mg vitamin C) mixed in cylindrical sample vial, the solution of 0.8 mL zinc chloride (mass ratio 1:2) dissolved in water synthesized was instilled in the mixture. Then, the vessel was placed in an electrical oven at 95 °C for 1h.

MOF-5: Terephthalic acid (3.05 mmol) and triethylamine (0.85 mL) was dissolved in 40 mL of DMF (denoted as solution A), Zn(NO₃)₂·6H₂O (77.4 mmol) was dissolved in 50 mL of DMF (denoted as solution B), then put solution A slowly into solution B under stirring, after 2.5 h at room temperature. The solution containing Zn²⁺ and organic were combined with stirring 2.5 h. The product was washed with DMF and CHCl₃ repeatedly.

MOF-199: Benzenetricarboxylic acid (4.76 mmol) was dissolved in a 1:1:1 mixture of 24 mL DMF/EtOH/H₂O (denoted as solution A). Cu²⁺ (8.62 mmol) was mixed with another 24 mL (denoted as solution B) and added in the prior solution. And then triethylamine was added. The product was washed with DMF repeatedly.

MIL-88-Fe: FeCl₃ (486 mg) and Terephthalic acid (332 mg) was dissolved in DMF (20 mL) in 100° for 12 h. The product was washed with ethanol repeatedly.

ZnO: $\text{Zn}(\text{CH}_3\text{COO})_2$ and Vc was dissolved in NaOH solution and stirred for homogeneous. And then heated at 100° for 6 h.

Fe₃O₄: 4.78 g of $\text{FeCl}_2 \cdot 4\text{H}_2\text{O}$ was dissolved in 12.5 mL of 12 M HCl, then the mixed solution was dropwised in 125 mL of 1.5 M NaOH solution under stirring, resulting in a brown precipitation.

GA: 12 mL GO aqueous solution (1 mg ml^{-1}) and 12 μL hydrazine hydrate mixed in cylindrical sample vial.

3. Supporting Figures

Figure S1. AFM image of GO layer (left), width of GO layer measured by AFM (right).

Figure S2. Nitrogen (at 77 K) adsorption desorption isotherms for rGA, ZIF-8/rGA samples

Figure S3. Characteristics of ZIF-8/rGA with reductant and without reductant under 95 °C for 1 h: (a) Wide-scan XPS spectra and (b) Raman spectrum and (d) FT-IR spectrum. (e) Normalized relative remaining mass measured by TGA analysis. Static contact angle of aerogel prepared without (c) and with (f) reductant.

Figure S4. Room temperature I-V matched curve of the aerogel without (a) and with (b) reductant representing ohmic characteristics, inset pictures showed the optical images of LED connected to aerogel under 3 V battery.

Figure S5. SEM and corresponding EDS mapping of rGA/Fe₃O₄.

Figure S6. Heat treatment solvent recycling.

Figure S7. a) Low-magnified FESEM images of ZIF-8/rGA after burning, b) high-magnified FESEM images of ZIF-8/rGA after burning, c) XRD of ZIF-8/rGA after burning, contact angle of ZIF-8/rGA after burning (inset of Figure S8 c).

Figure S8. a) The original solution, b) rGA, c) and d) ZIF-8/rGA adsorbed for 4, 8 h in dark, e and f) ZIF-8/rGO, ZIF-8/rGA after adsorbing 8 h transferred to photocatalysis in 10 min, g) adsorption and photocatalysis.

4. Supporting Table

Table S1. Fabrication methods and efficiency comparison of pure rGA and rGA composites.

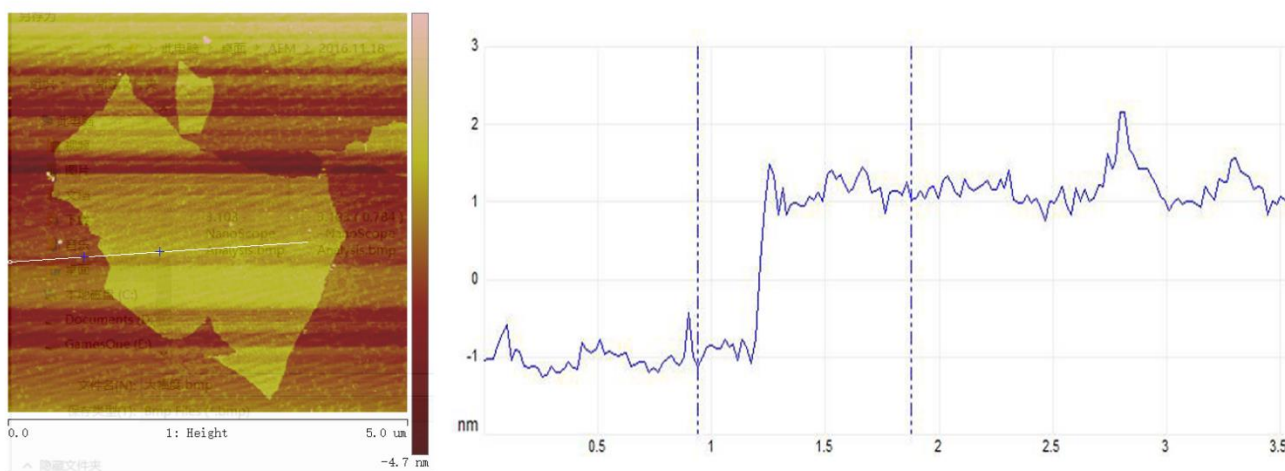


Figure S1. AFM image of GO layer (left), width of GO layer measured by AFM (right). From the AFM pictures, the thickness of GO is around 2 nm and GO is composed of 2 monolayers.

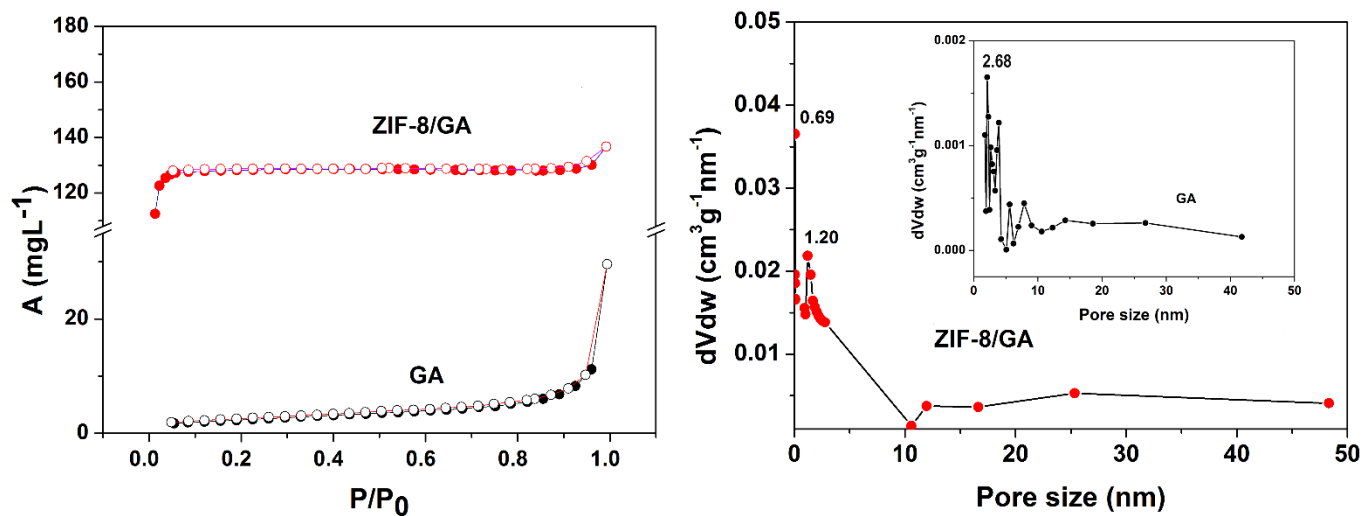


Figure S2. Nitrogen (at 77 K) adsorption-desorption isotherms for rGA, rGA/ZIF-8 samples. The BET surface area of the rGA sample was around $\sim 16 \text{ m}^2 \text{ g}^{-1}$, and ZIF-8 adding immensely increased BET surface area to $\sim 168 \text{ m}^2 \text{ g}^{-1}$. BJH Adsorption average pore diameter was 1.74 nm and adsorption average pore width was 5.1 nm. Adsorbability enhanced along with the BET surface area may remove more contaminant. Due to ZIF-8, aerogel can be used to significant CO_2 uptake or gas separation.

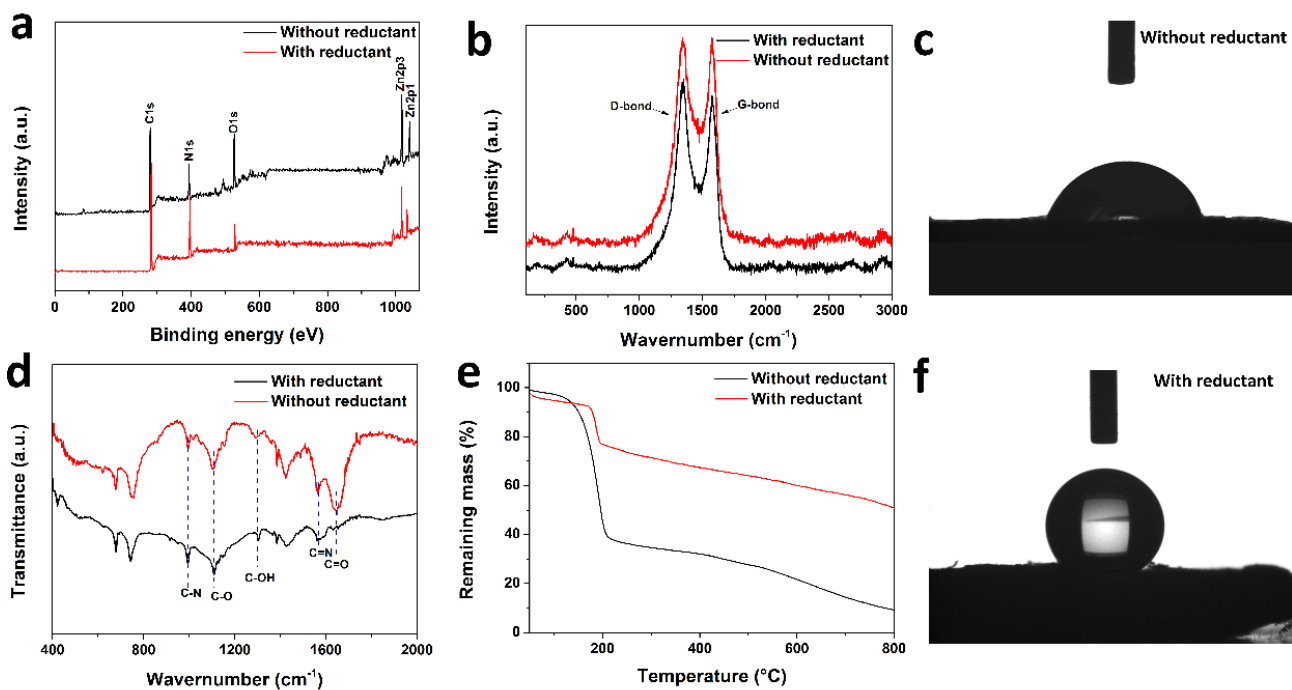


Figure S3. Characteristics of rGA/ZIF-8 with reductant and without reductant under 95 °C for 1 h: (a) Wide-scan XPS spectra and (b) Raman spectrum and (d) FT-IR spectrum. (e) Normalized relative remaining mass measured by TGA analysis. Static contact angle of aerogel prepared without (c) and with (f) reductant. Wide-scan XPS spectra, Raman spectrum, FT-IR spectrum illustrated that Hydrazine hydrate and other reductants help more effective reduction of GO, which will effectively improve performances of aerogel (such as thermostability and hydrophobicity).

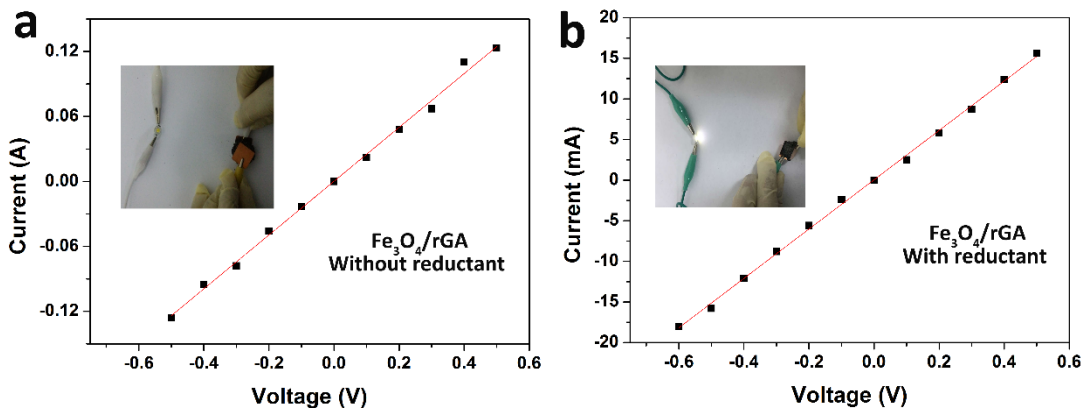


Figure S4. Room temperature I-V matched curve of the aerogel without (a) and with (b) reductant representing ohmic characteristics, inset pictures showed the optical images of LED connected to aerogel under 3 V battery. When a LED lamps connected to the rGA/Fe₃O₄ without reductant, the LED lamps can't be lighted. In addition to the excellent apparent promotion of thermos-stability and hydrophobicity, electrically conductive has greatly improved when reductant adding. A LED lamps connected to the rGA/Fe₃O₄ without reductant, rGA/Fe₃O₄ under 3 V displayed ohmic drop from 4000 to 35, indicating an outstanding conductive performance for many practical applications. π -conjugated system recovery from GO layers upon hydrazine hydrate reduction is mainly reason contributing to attractive electrically conductive such as pressure-responsive sensors.

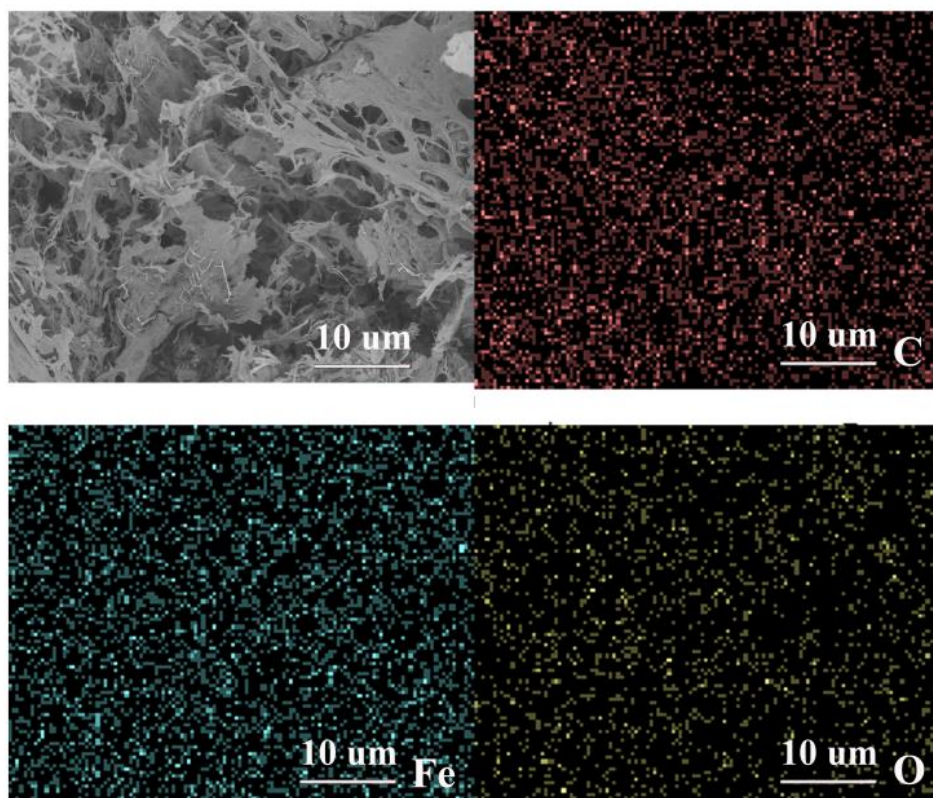


Figure S5. SEM and corresponding EDS mapping of rGA/Fe₃O₄. rGA/Fe₃O₄ has porous structure displayed by SEM picture and the uniformly elements from EDS mapping showed Fe₃O₄ has been successfully deposited on the GO layer walls.

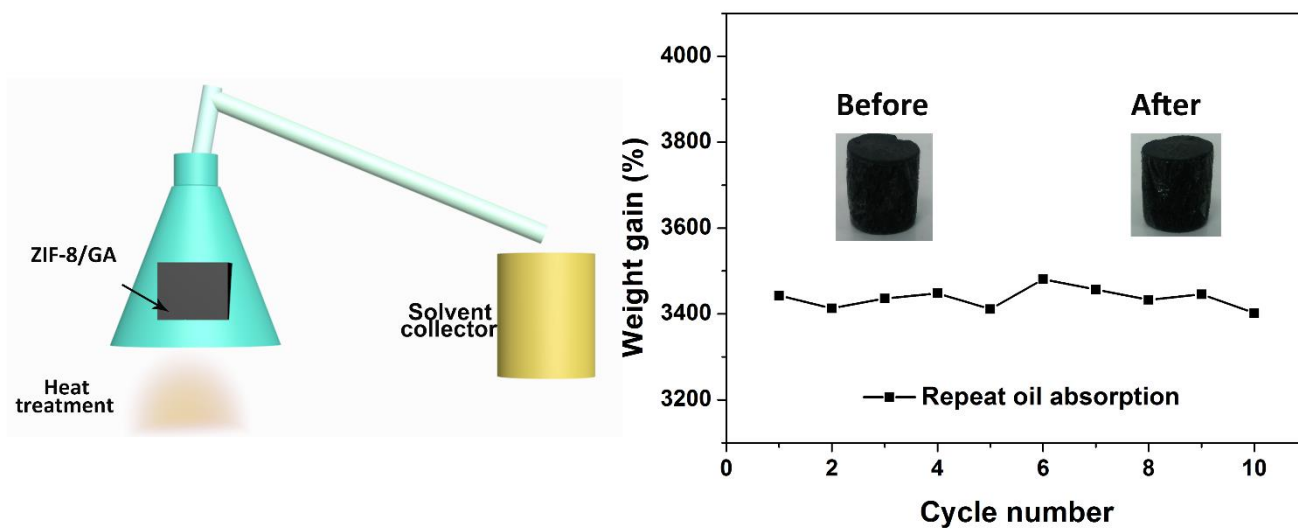


Figure S6. Heat treatment solvent recycling. Precious volatile solvent adsorbed by ZIF-8/rGA can be gathered by distilling with recycle stability

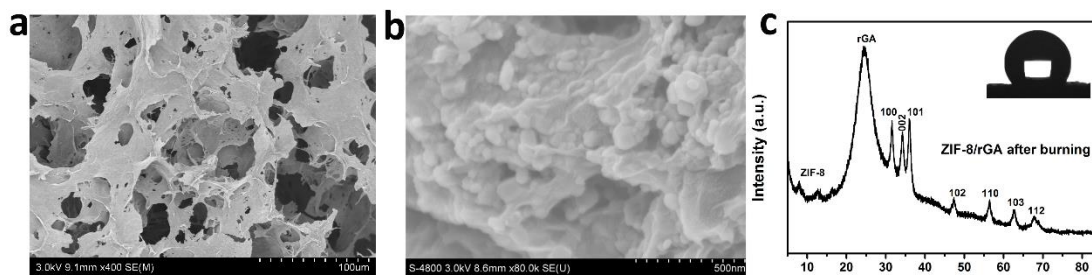


Figure S7. a) Low-magnified FESEM images of ZIF-8/rGA after burning, b) high-magnified FESEM images of ZIF-8/rGA after burning, c) XRD of ZIF-8/rGA after burning, contact angle of ZIF-8/rGA after burning (inset of Figure S8 c). The ZIF-8 from ZIF-8/rGA partially burning into ZnO, while the aerogel maintaining with the 3D porous frameworks and the contact angle was 138.6°.

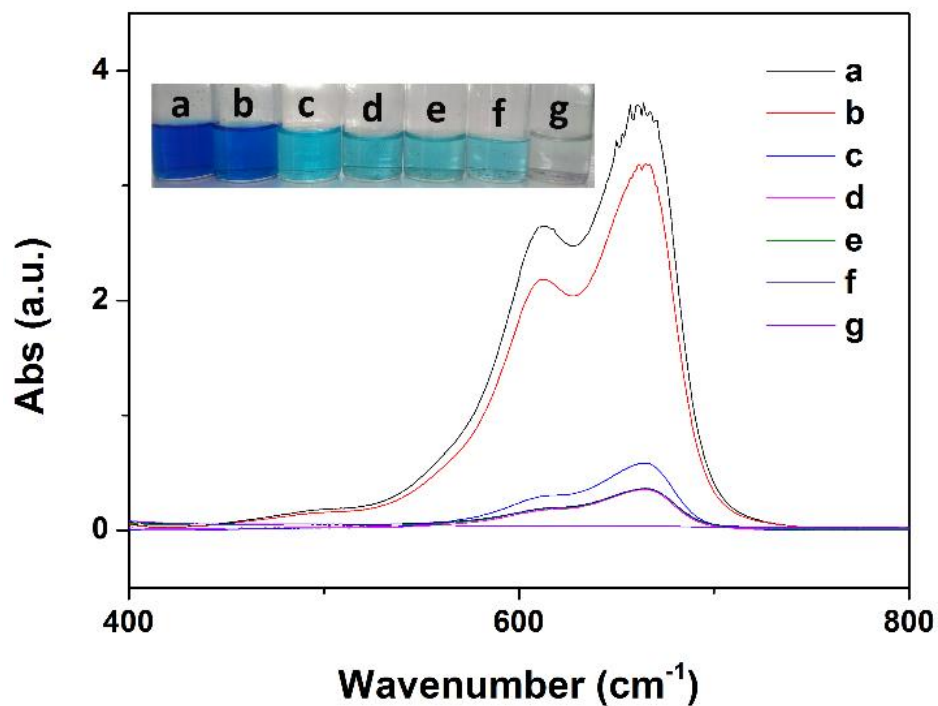


Figure S8. a) The original solution, b) rGA, c) and d) ZIF-8/rGA adsorbed for 4, 8 h in dark, e and f) ZIF-8/GO, ZIF-8/rGA after adsorbing 8 h transferred to photocatalysis in 10 min, g) adsorption and photocatalysis. Optical images and UV-Vis absorption spectrometer show efficient photocatalytic degradation of ZIF-8/rGA.

Table S1: Fabrication methods and efficiency comparison of pure rGA and rGA composites.

	Gel formation	Oil-water separation	Heavy metals (mg g ⁻¹)	Photodegradation	Organic pollutants (mg g ⁻¹)	Ref.
GA	12-24 h	20-86 times	/	/	/	1,2
PDA/GA	6-12 h	26-42.5 times	100-320	/	89-360	3,4
AgX/GA	12 h	/	/	yes	/	5
α -FeOOH/GA	6 h	13-28 times	139-374	/	/	6
Tannic Acid/GA	8 h	15-30 times	/	/	75-380	7
PtNPs/GA	3 h	/	/	yes	30-660	8
CNTs/GA	6 h	/	/	/	626 (MB)	9
PVA/GA	10 h	20-70	/	/	/	10
AgCS/GA	9 h	/	13	yes	65.8 (MB)	11
ZIF-8/GA	1 h	34-59 times	61-250	yes	220 (H ₂ -PA)	This work

Compare to rGA or rGA composites published before, we firstly reported a novel and rapid strategy for the rational construction of stably, highly porous and multifunctional MOFs@rGA hydrogel composites at 95° within a short time (< 1 h). Besides, MOFs@rGA hydrogel exhibited excellent multifunction for the oil absorption, photocatalytic dye degradation and water resource reclamation.

- 1 Y. X. Xu, K. X. Sheng, C. Li and G. Q. Shi, *ACS Nano.*, 2010, **4**, 4324-4330.
- 2 H. Bi, X. Xie, K. Yin, Y. Zhou, S. Wan, L. He, F. Xu, F. Banhart, L. Sun and R. S. Ruoff, *Adv. Funct. Mater.*, 2012, **22**, 4421-4425.
- 3 C. Cheng, S. Li, J. Zhao, X. Li, Z. Liu, L. Ma, X. Zhang, S. Sun and C. Zhao, *Chem. Eng. J.* 2013, **228**, 468-481.
- 4 H. Gao, Y. Sun, J. Zhou, R. Xu and H. Duan, *ACS Appl. Mater. Inter.*, 2013, **5**, 425-432.
- 5 Y. Y. Fan, W. G. Ma, D. X. Han, S. Y. Gan, X. D. Dong and L. Niu, *Adv. Mater.*, 2015, **27**, 3767-3773.
- 6 H. P. Cong, X. C. Ren, P. Wang and S. H. Yu, *ACS Nano*, 2012, **6**, 2693-2703.
- 7 J. Luo, J. P. Lai, N. Zhang, Y. B. Liu, R. Liu and X. Y. Liu, *ACS Sustain. Chem. Eng.*, 2016, **4**, 1404-1413.
- 8 X. P. Zhang, D. Liu, L. Yang, L. M. Zhou and T. Y. You, *J Mater. Chem. A*, 2015, **3**, 10031-10037.
- 9 B. Lee, S. Lee, M. Lee, D. H. Jeong, Y. Baek, J. Yoon and Y. H. Kim, *Nanoscale*, 2015, **7**, 6782-6789.
- 10 R. Li, C. B. Chen, J. Li, L. M. Xu, G. Y. Xiao and D. Y. Yan, *J. Mater. Chem. A*, 2014, **2**, 3057-3064.

11 S. P. Dubey, A. D. Dwivedi, I. C. Kim, M. Sillanpaa, Y. N. Kwon and C. Lee,
Chem. Eng. J., 2014, **244**, 160-167.